Webster, J.M., Ravelo, A.C., Grant, H.L.J., and the Expedition 389 Scientists
Proceedings of the International Ocean Discovery Program Volume 389
publications.iodp.org

Site M0106[1]

J.M. Webster, A.C. Ravelo, H.L.J. Grant, M. Rydzy, M. Stewart, N. Allison, R. Asami, B. Boston, J.C. Braga, L. Brenner, X. Chen, P. Chutcharavan, A. Dutton, T. Felis, N. Fukuyo, E. Gischler, S. Greve, A. Hagen, Y. Hamon, E. Hathorne, M. Humblet, S. Jorry, P. Khanna, E. Le Ber, H. McGregor, R. Mortlock, T. Nohl, D. Potts, A. Prohaska, N. Prouty, W. Renema, K.H. Rubin, H. Westphal, and Y. Yokoyama[2]

[1] Webster, J.M., Ravelo, A.C., Grant, H.L.J., Rydzy, M., Stewart, M., Allison, N., Asami, R., Boston, B., Braga, J.C., Brenner, L., Chen, X., Chutcharavan, P., Dutton, A., Felis, T., Fukuyo, N., Gischler, E., Greve, S., Hagen, A., Hamon, Y., Hathorne, E., Humblet, M., Jorry, S., Khanna, P., Le Ber, E., McGregor, H., Mortlock, R., Nohl, T., Potts, D., Prohaska, A., Prouty, N., Renema, W., Rubin, K.H., Westphal, H., and Yokoyama, Y., 2025. Site M0106. In Webster, J.M., Ravelo, A.C., Grant, H.L.J., and the Expedition 389 Scientists, Hawaiian Drowned Reefs. Proceedings of the International Ocean Discovery Program, 389: College Station, TX (International Ocean Discovery Program). https://doi.org/10.14379/iodp.proc.389.113.2025

[2] **Expedition 389 Scientists' affiliations.**

Contents

Keywords
International Ocean Discovery Program, IODP, Expedition 389, *MMA Valour*, Hawaiian Drowned Reefs, Earth climate system, Earth system feedbacks, Earth history tipping points, Site M0106, coral reef, volcanics, sea level, paleoclimate, central Pacific, reef health, Hawaiian geology, basalt, lava, carbonates, Ka Lae

Core descriptions

Supplementary material

References (RIS)

MS 389-113
Published 26 February 2025

Funded by ECORD, JAMSTEC, and NSF OCE1326927

1. Operations

The multipurpose vessel *MMA Valour* was used as the drilling platform throughout Expedition 389. At all Expedition 389 sites, dynamic positioning was used to provide accurate positions throughout operations and water depth was established using a Sound Velocity Profiler (SVP) placed on the top of the PROD5 drilling system. For more detail on acquisition methods, see **Introduction** in the Expedition 389 methods chapter (Webster et al., 2025a).

Summary operational information for Site M0106 is provided in Table **T1**. All times stated are in Hawaiian Standard Time (HST).

1.1. Hole M0106A

The *MMA Valour* arrived on location at 2235 h on 17 October 2023, and PROD5 was deployed at 2236 h. The seabed at the original target location appeared to be characterized by basaltic outcrops, so PROD5 was moved 100 m southeast at a bearing of 137° and a water depth of 148.6 m. Coring commenced in Hole M0106A and reached 7.41 meters below seafloor (mbsf) at 0514 h on 18 October, when a seal failure on the drive head meant PROD5 had to be recovered and the hole was terminated. PROD5 was returned to deck at 0602 h, when on-deck operations commenced, core barrels were extracted for curation, and repairs were undertaken.

A total of four cores were recovered from Hole M0106A from 7.43 m of rotary coring. The total recovered core length was 1.47 m (19.78% recovery).

Table T1. Hole summary, Site M0106. R = rotary coring mode. LAT = Lowest Astronomical Tide. **Download table in CSV format.**

Hole	Water depth (mbsf)	Date started (2023)	Date finished (2023)	Latitude	Longitude	Coring method	Total drilled depth (m)	Recovered length (m)	Core recovery (%)	Cores (*N*)	Notes
389-											
M0106A	148.6	17 Oct	18 Oct	18.856679°	−155.688330°	R	7.43	1.47	20	4	LAT water depth: 148.1 m. Borehole terminated due to technical issues.
M0106B	147.9	18 Oct	19 Oct	18.856772°	−155.688265°	R	16.14	2.98	32	10	LAT water depth: 147.4 m. Borehole terminated as per client request. Casing abandoned due to issues recovering the string.

1.2. Hole M0106B

PROD5 was redeployed at Site M0106 at a water depth of 147.9 m at 0945 h on 18 October 2003 following repairs. Starting at 1015 h, Hole M0106B was wash bored to 7.00 mbsf, just above the final depth of Hole M0106A. Rotary coring and casing commenced at 1300 h on 18 October. Difficulties were encountered in attempting to set casing in Hole M0106B, likely caused by the presence of sand and gravel, which stalled casing at 15.62 mbsf. Wash boring was attempted from 15.62 to 16.11 mbsf, but initial attempts to recover the wash bore failed with problems at 10.70 mbsf. When the wash bore was recovered and the casing was pulled, it was discovered that the casing had parted, leaving three casing sections and the spud casing downhole. The borehole was terminated at 0815 h on 19 October. PROD5 was recovered to deck at 0855 h, on-deck operations commenced, and core barrels were extracted for curation. The transit back to Site M0099 began at 1028 h on 19 October.

A total of 10 cores were recovered from Hole M0106B from 9.26 m of rotary coring (6.88 m of wash boring). The total recovered core length was 2.98 m (32.18% recovery).

2. Lithostratigraphy

Holes M0106A and M0106B are located in the Ka Lae region (South Point) at 148.6 and 147.9 meters below sea level (mbsl), respectively. Core material recovered from Site M0106 (Figure **F1**) consists mostly of loose rhodoliths with crustose and fruticose coralline algal crusts down to 11.50 mbsf. Below this depth in Hole M0106B, a 1.30 m section of unconsolidated biodetrital sediment containing pebble-sized rhodoliths and coral clasts in a finer bioclastic matrix overlies a coralgal boundstone with massive *Porites*.

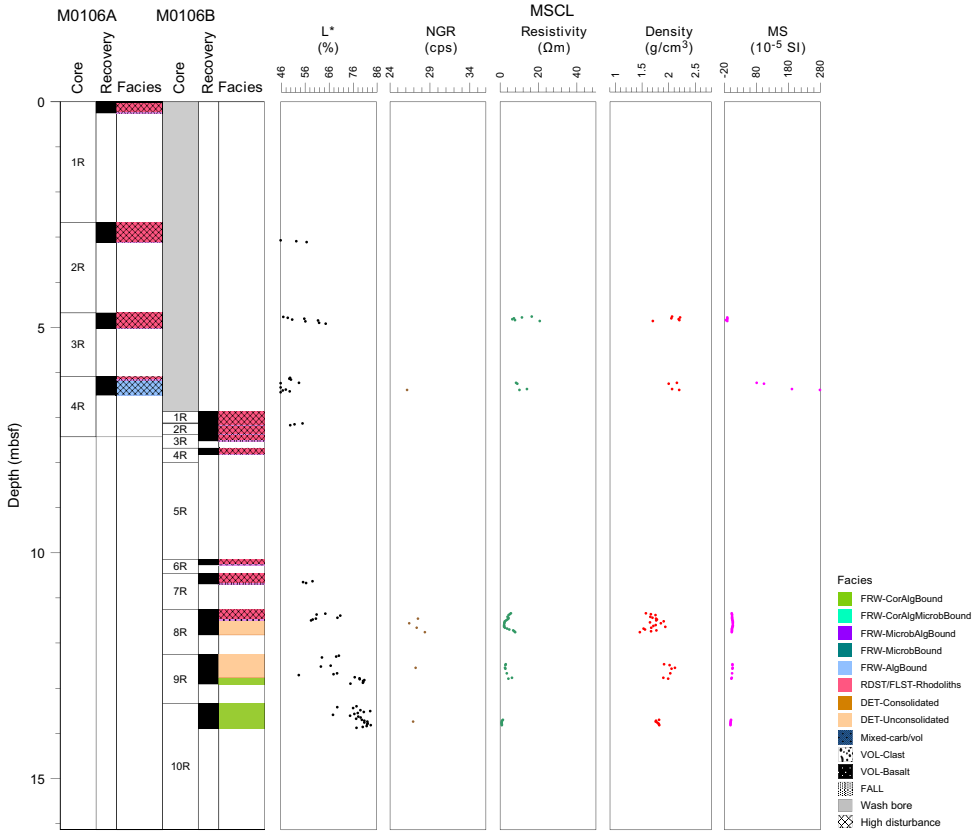

Figure F1. Composite lithostratigraphy, Holes M0106A and M0106B. cps = counts per second, MS = magnetic susceptibility.

2.1. Holes M0106A and M0106B

Holes M0106A and M0106B represent a composite hole and are described together.

In Hole M0106A (Figure **F2**), the recovered core material from 0 to 6.16 mbsf (Figure **F3A**) consists of loose rhodoliths formed by crustose and fruticose coralline algal crusts that vary in size and are up to 12 cm in diameter. Rhodolith nuclei include coral fragments (e.g., *Porites* and *Cyphastrea*). Loose coral branches and *Montipora* clasts are present in the sediment between rhodoliths. The lowermost part of the core, from 6.16 to 6.51 mbsf, is composed of algal boundstone containing a *Montipora* colony (Figure **F3B**).

Hole M0106B (Figure **F4**) was wash bored to the approximate final depth of Hole M0106A and then cored to 13.90 mbsf. Core material from 6.86 to 11.49 mbsf is composed of loose rhodoliths formed by crustose and fruticose coralline algal crusts, varying between 1 and 7 cm in diameter (Figure **F5A**). From 11.49 to 12.77 mbsf, the core consists of unconsolidated biodetrital sediment containing pebble-sized rhodoliths and coral clasts (*Porites* and *Pocillopora*) encrusted with coralline algae embedded in a finer bioclastic matrix composed of mollusk shells, foraminifers, and

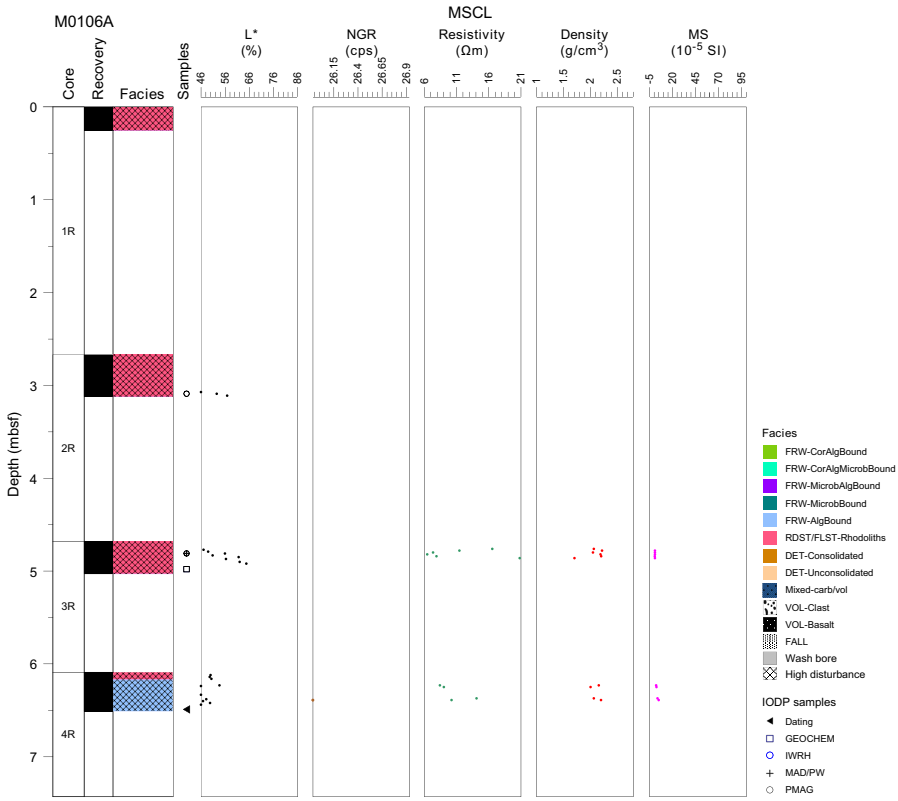

Figure F2. Lithostratigraphy and MSCL data, Hole M0106A. cps = counts per second, MS = magnetic susceptibility.

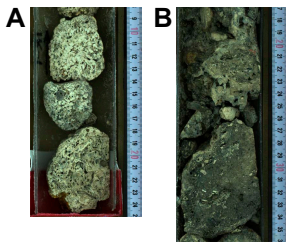

Figure F3. Facies, Hole M0106A. A. Rhodoliths (1R-1, 8–25 cm). B. Algal boundstone (4R-1, 17–36 cm).

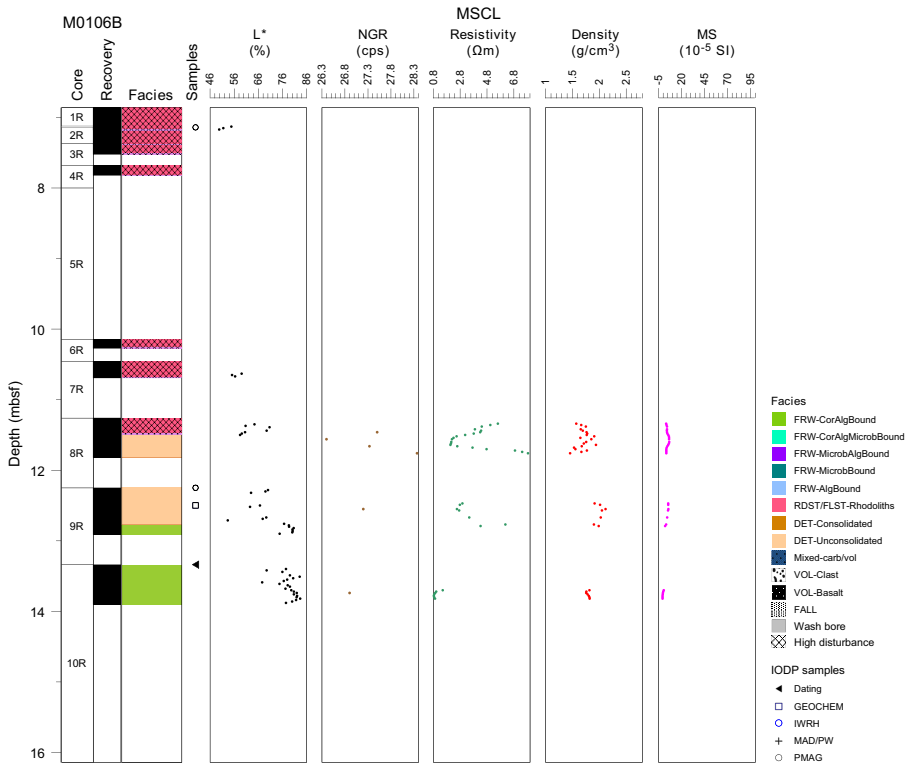

Figure F4. Lithostratigraphy and MSCL data, Hole M0106B. cps = counts per second, MS = magnetic susceptibility.

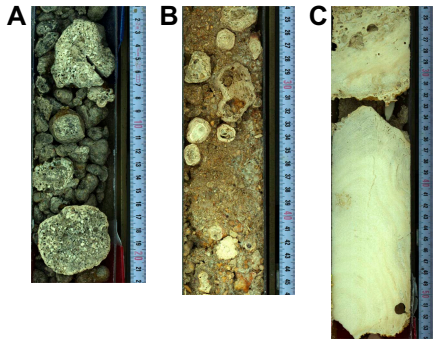

Figure F5. Facies, Hole M0106B. A. Rhodoliths (7R-1, 1–22 cm). B. Unconsolidated biodetrital sediment containing rhodoliths and bioclasts (8R-1, 24–46 cm). C. Coralgal boundstone with massive *Porites* (10R-1, 24–54 cm).

echinoid spines (Figure F5B). A coralgal boundstone with massive *Porites* colonies, partly fragmented during coring, was recovered from 12.77 mbsf to the bottom of the hole at 13.90 mbsf (Figure F5C).

3. Physical properties

Physical properties data for Site M0106 are shown in Table T2 in the Site M0096 chapter (Webster et al., 2025b).

3.1. Hole M0106A

A total of 0.77 m of core from Hole M0106A was scanned with the multisensor core logger (MSCL), and because the core exhibited major drilling-induced disturbance, only 31% of the acquired data passed QA/QC (see Table T10 in the Expedition 389 methods chapter [Webster et

al., 2025a]). One discrete sample was taken for *P*-wave velocity and moisture and density (MAD) measurements. Digital linescans, color reflectance, and hyperspectral imaging were acquired on all cores.

3.1.1. Density and porosity

Data for density and porosity measurements are presented in Figures **F2** and **F6**. MSCL bulk density values range 1.71–2.22 g/cm^3. Drilling-induced disturbance and short core lengths compromised data quality (see **Physical properties** in the Expedition 389 methods chapter [Webster et al., 2025a]) and limited sampling. One discrete sample was analyzed for MAD, giving a bulk density value of 2.29 g/cm^3. The porosity value for this sample is 25.7%, and the grain density value is 2.732 g/cm^3.

3.1.2. *P*-wave velocity

MSCL *P*-wave velocity measurements yielded no data. One sample was measured using the discrete *P*-wave logger. The dry *P*-wave velocity value is 3892 m/s (Figure **F7**). The *P*-wave velocity measured for the resaturated sample is 4448 m/s. Because of the limited *P*-wave data, it is not possible to discern downhole trends.

3.1.3. Thermal conductivity

Because of the presence of drilling-induced disturbances, large voids, and uneven surfaces, thermal conductivity measurements were not performed.

3.1.4. Magnetic susceptibility

MSCL magnetic susceptibility data range 0.67 × 10^{-5} to 4.99 × 10^{-5} SI (Figure **F2**). The majority of magnetic susceptibility values are close to 1.87 × 10^{-5} SI. There are no downhole trends.

3.1.5. Electrical resistivity

MSCL noncontact resistivity measurements range 6.45–20.80 Ωm (Figure **F2**). Similar to the other data sets for this hole, it is difficult to discern trends or notable features.

3.1.6. Natural gamma radiation

A single MSCL natural gamma radiation (NGR) measurement has a value of 26 counts/s (Figure **F2**).

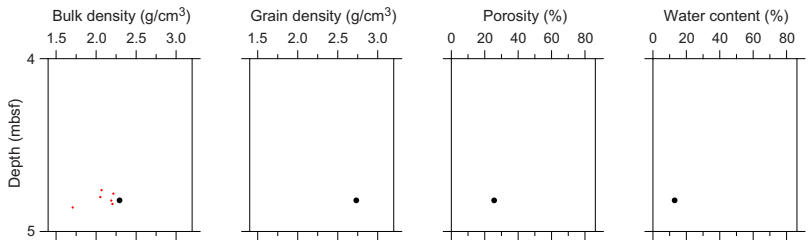

Figure F6. Physical properties, Hole M0106A. Black = discrete sample, red = MSCL.

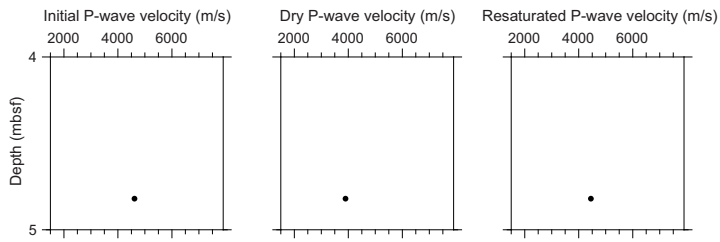

Figure F7. Initial, dry, and resaturated *P*-wave velocities measured on one discrete sample, Hole M0106A.

3.1.7. Digital linescans, color reflectance, and hyperspectral imaging

All cores were digitally scanned, measured for color reflectance (where appropriate), and imaged with the hyperspectral scanner (see HYPERSPECTRAL in **Supplementary material**). Color reflectance L* values vary between 35.93% and 64.79%, a* varies between –1.02 and 1.77, b* varies between 4.48 and 14.10, and a*/b* varies between –0.23 and 0.14. (Figure **F2**).

3.2. Hole M0106B

A total of 1.78 m of core from Hole M0106B was scanned with the MSCL, and the core exhibited moderate drilling-induced disturbance, resulting in 59% of the acquired data passing QA/QC (see Table **T10** in the Expedition 389 methods chapter [Webster et al., 2025a]). No discrete samples were taken for *P*-wave velocity and MAD measurements. Digital linescans, color reflectance, and hyperspectral imaging were acquired on all cores.

3.2.1. Density and porosity

Data for density and porosity measurements are presented in Figure **F4**. MSCL bulk density values range 1.46–2.12 g/cm^3. The core quality and the short core lengths compromised the data quality and prohibited sampling (see **Physical properties** in the Expedition 389 methods chapter [Webster et al., 2025a]).

3.2.2. *P*-wave velocity

MSCL *P*-wave velocity measurements yielded no data. Because of poor core quality, no samples were collected for discrete *P*-wave velocity measurements.

3.2.3. Thermal conductivity

No thermal conductivity data were collected for Hole M0106B.

3.2.4. Magnetic susceptibility

MSCL magnetic susceptibility data range -0.73×10^{-5} to 6.59×10^{-5} SI (Figure **F4**) with mean values close to 3.60×10^{-5} SI.

3.2.5. Electrical resistivity

MSCL noncontact resistivity measurements range 0.84–7.85 Ωm (Figure **F4**). Similar to other data sets for this hole, it is difficult to discern any downcore trends in resistivity data due to poor core recovery.

3.2.6. Natural gamma radiation

MSCL NGR measurements range 26–28 counts/s (Figure **F4**) and show no apparent downhole trend.

3.2.7. Digital linescans, color reflectance, and hyperspectral imaging

All cores were digitally scanned, measured for color reflectance (where appropriate), and imaged with the hyperspectral scanner (see HYPERSPECTRAL in **Supplementary material**). Color reflectance L* values vary between 49.79% and 83.32%, a* varies between 0.09 and 4.65, b* varies between 11.47 and 24.14, and a*/b* varies between 0.01 and 0.20 (Figure **F4**). Increasing L* values at 11.50 mbsf seem to correspond to a change in carbonate facies from rhodolith-rich sediment to coralgal boundstone.

4. Geochemistry

4.1. Interstitial water

No interstitial water samples were collected from Site M0106.

Table T2. HighScore X-ray diffraction (XRD) mineral abundances, Site M0106. **Download table in CSV format.**

Table T3. Solid-phase elemental abundances, Site M0106. **Download table in CSV format.**

Table T4. TOC, TIC, and TC, Site M0106. **Download table in CSV format.**

4.2. Surface seawater

A surface seawater sample was collected from Site M0106 using a Niskin bottle deployed from the side of the vessel (see Figure **F22** in the Expedition 389 methods chapter [Webster et al., 2025a]). The salinity, pH, alkalinity, ammonium, and major element chemistry measured for this sample are consistent with the other surface seawater samples taken during Expedition 389 and align with the expected values for conservative elements in seawater (see Tables **T15** and **T17** in the Expedition 389 methods chapter [Webster et al., 2025a]).

4.3. Bulk sediment and rocks

Two bulk sediment samples were taken from Hole M0106A (Figure **F2**) and analyzed for mineralogy, elemental composition, and carbon content. The samples are derived from a rhodolith and a mixed carbonate-volcaniclastic sediment interval.

4.4. Mineralogy

Samples from Site M0106 consist of high-Mg calcite and aragonite mineral phases (Table **T2**). The rhodolith sample from 4.98 mbsf (389-M0106A-3R-1, 30–32 cm) is composed of two thirds high-Mg calcite (68%) and one third (32%) aragonite. The mixed carbonate-volcaniclastic sediment sample from 12.50 mbsf (389-M0106B-9R-1, 25–29 cm) is composed of 45% high Mg-calcite and 53% aragonite.

4.5. Elemental abundances

The concentrations of major elements in the carbonate samples from Site M0106 reflect the carbonate material analyzed (Table **T3**). Iron is present in both samples and the mixed carbonate-volcaniclastic sediment sample from 12.50 mbsf (389-M0106B-9R-1, 25–29 cm) also has detectable amounts of P, Ti, Ni, Cr, and Rb.

4.6. Carbon content

The results for total organic carbon (TOC), total carbon (TC), and total inorganic carbon (TIC) at Site M0106 are presented in Table **T4**. TC content is 11.3% in both samples, whereas TOC content is low at 0.16% and 0.19% and $CaCO_3$ content is very high at above 92% (>11.1% TIC) (see GEOCHEM in **Supplementary material** for calculated $CaCO_3$ values).

5. Paleomagnetism

Four samples were obtained from Holes M0106A and M0106B. Measurements of low-field and mass-specific magnetic susceptibility (χ) were carried out for all samples. The initial natural remanent magnetization (NRM) was measured for all samples, as well as NRM following stepwise alternating field (AF) demagnetization up to a peak AF of 20 mT. For further details, see **Paleomagnetism** in the Expedition 389 methods chapter (Webster et al., 2025a). Paleomagnetism data for Site M0106 is shown in Table **T5**.

Table T5. Magnetic susceptibility and NRM, Site M0106. **Download table in CSV format.**

Core, section, interval (cm)	Sample type	Depth (mbsf)	Magnetic susceptibility (m^3/kg)	Initial NRM intensity (A/m)
389-M0106A-				
2R-1, 42–44	Carbonate	3.10	2.57×10^{-7}	2.24×10^{-3}
3R-1, 13–15	Carbonate	4.82	8.76×10^{-9}	5.38×10^{-4}
389-M0106B-				
1R-1, 28–30	Microbialite	7.15	1.68×10^{-7}	5.17×10^{-3}
9R-1, 0–4	Coralline	12.27	1.78×10^{-7}	7.03×10^{-3}

5.1. Hole M0106A

Two carbonate samples were taken at 3.10 mbsf (Sample 389-M0106A-2R-1, 42–44 cm) and 4.82 mbsf (Sample 3R-1, 13–15 cm). The χ values of the samples are 2.57×10^{-7} and 8.76×10^{-9} m^3/kg, respectively, and the initial NRM intensities are 2.24×10^{-4} and 5.38×10^{-4} A/m, respectively.

5.2. Hole M0106B

Two carbonate samples were taken from 7.14 mbsf (Sample 389-M0106B-1R-1, 28–30 cm) and 12.25 mbsf (Sample 9R-1, 0–4 cm). The χ values of the sample are 1.68×10^{-7} and 1.78×10^{-7} m^3/kg, and the initial NRM intensities are 5.17×10^{-3} and 7.03×10^{-3} A/m, respectively.

6. Geochronology

Two radiocarbon dates were obtained from Site M0106: Samples 389-M0106A-4R-1, 40–41 cm, and 389-M0106B-10R-1, 0–2 cm. The uncalibrated dates range 28–35 ^{14}C ky BP (see Table **T23** in the Expedition 389 methods chapter [Webster et al., 2025a]). The dates are consistent with the interpretation of the age of the H1 terrace spanning Marine Isotope Stages 1–5 (Webster et al., 2009; Ludwig et al., 1991).

References

Ludwig, K.R., Szabo, B.J., Moore, J.G., and Simmons, K.R., 1991. Crustal subsidence rate off Hawaii determined from $^{234}U/^{238}U$ ages of drowned coral reefs. Geology, 19(2):171–174. **https://doi.org/10.1130/0091-7613(1991)019<0171:CSROHD>2.3.CO;2**

Webster, J.M., Braga, J.C., Clague, D.A., Gallup, C., Hein, J.R., Potts, D.C., Renema, W., Riding, R., Riker-Coleman, K., Silver, E., and Wallace, L.M., 2009. Coral reef evolution on rapidly subsiding margins. Global and Planetary Change, 66(1–2):129–148. **https://doi.org/10.1016/j.gloplacha.2008.07.010**

Webster, J.M., Ravelo, A.C., Grant, H.L.J., and the Expedition 389 Scientists, 2025. Supplementary material, **https://doi.org/10.14379/iodp.proc.389supp.2025**. In Webster, J.M., Ravelo, A.C., Grant, H.L.J., and the Expedition 389 Scientists, Hawaiian Drowned Reefs. Proceedings of the International Ocean Discovery Program, 389: College Station, TX (International Ocean Discovery Program).

Webster, J.M., Ravelo, A.C., Grant, H.L.J., Rydzy, M., Stewart, M., Allison, N., Asami, R., Boston, B., Braga, J.C., Brenner, L., Chen, X., Chutcharavan, P., Dutton, A., Felis, T., Fukuyo, N., Gischler, E., Greve, S., Hagen, A., Hamon, Y., Hathorne, E., Humblet, M., Jorry, S., Khanna, P., Le Ber, E., McGregor, H., Mortlock, R., Nohl, T., Potts, D., Prohaska, A., Prouty, N., Renema, W., Rubin, K.H., Westphal, H., and Yokoyama, Y., 2025a. Expedition 389 methods. In Webster, J.M., Ravelo, A.C., Grant, H.L.J., and the Expedition 389 Scientists, Hawaiian Drowned Reefs. Proceedings of the International Ocean Discovery Program, 389: College Station, TX (International Ocean Discovery Program). **https://doi.org/10.14379/iodp.proc.389.102.2025**

Webster, J.M., Ravelo, A.C., Grant, H.L.J., Rydzy, M., Stewart, M., Allison, N., Asami, R., Boston, B., Braga, J.C., Brenner, L., Chen, X., Chutcharavan, P., Dutton, A., Felis, T., Fukuyo, N., Gischler, E., Greve, S., Hagen, A., Hamon, Y., Hathorne, E., Humblet, M., Jorry, S., Khanna, P., Le Ber, E., McGregor, H., Mortlock, R., Nohl, T., Potts, D., Prohaska, A., Prouty, N., Renema, W., Rubin, K.H., Westphal, H., and Yokoyama, Y., 2025b. Site M0096. In Webster, J.M., Ravelo, A.C., Grant, H.L.J., and the Expedition 389 Scientists, Hawaiian Drowned Reefs. Proceedings of the International Ocean Discovery Program, 389: College Station, TX (International Ocean Discovery Program). **https://doi.org/10.14379/iodp.proc.389.103.2025**